CrossMark

Optical and electrical properties of fluorine doped tin oxide thin film

E. Ching-Prado[1] · A. Watson[1] · H. Miranda[1]

Abstract

Thin film of SnO_2:F was prepared by spray pyrolysis technique on glass substrate. Surface Morphology, using scanning electron microscope, shows micrograph image with grains size distribution between 16 and 380 nm. Structural characterization by XRD indicates a similar rutile polycrystalline material as SnO_2. A four point probe I–V measurement (Van der Pauw method) was used to study electrical properties and the result shows a room temperature sheet resistance of 24 Ω/sq. In addition, a temperature dependence of the electrical response indicates that defect scattering is the main contribution to the DC resistivity. Optical properties were studied by UV–Visible spectroscopy and the spectrum was fitted using Drude-Lorentz model with DC conductivity value (frequency equal to zero) as a fitting condition. Optical result shows average transmittance around 81.2% for the visible frequency range. It indicates a TCO figure of merit value of 5.2×10^{-3} $Ω^{-1}$. In addition, a first principle calculation using DFT with PBE0 hybrid exchange-correlation was realized to SnO_2 and SnO_2:F systems in order to understand, from a theoretical point of view, the experimental results. Finally, the FTO film was utilized and evaluated as a transparent electrode in the preparation of a dye-sensitized solar cell.

1 Introduction

Tin oxide is a functional material used in many applications, such as transparent conducting electrodes in solar cell, gas sensor, electrochromic devices, etc. Tin oxide is a crystalline solid with a tetragonal lattice structure similar to that of rutile. It is a n-type semiconductor material with direct wide band gap energy around 3.62 eV. Tin oxide has been doped with different chemical elements, such as F, In, Sb, Fe, and many others, in order to improve different physical properties [1, 2]. Fluorine doped tin oxide (FTO) is one of the most popular transparent conducting oxide (TCO) whose low resistivity strongly depends of the high carrier concentration produced by oxygen vacancy and the quantity of substitution fluorine. FTO thin film has been prepared by different experimental techniques, such as reactive sputtering, chemical vapor deposition (CVD), electrospun and spray pyrolysis (SP). The latter is a simple and cost effective technique applicable for large deposition area and with a good quality thin film as resulted [3–7].

In order to use FTO as a TCO semiconductor material for optoelectronic applications, accurate determination of several important parameters, such as complex permittivity, refraction index (n), extinction coefficient (k) and electrical resistivity is a fundamental requirement [8–13]. In the case of optical properties of semiconductors, important research works have been realized in order to find theoretical expressions [14]. Thus, the Drude model together with others optical models have been utilized to simulate experimental UV–Visible spectra of some TCO materials. For example, Drude and Lorentz models have been used to explain transmittance and reflectance spectra of CVD tin oxide (TO) and antimony-doped TO thin films [15]. In similar form, Drude and Kim oscillator models have been employed in the study of SP palladium-doped TO thin films [16]. Also, a combination of Drude and Forouhi–Bloomer models has been used to simulate the transmittance spectra of magnetron sputtered and electron beam evaporated indium tin oxide (ITO) thin films [17].

In the case of electrical response of TCO semiconductor materials, most of the research works invoke Bloch–Grüneisen (BG) law to explain the resistivity temperature dependence behavior [18]. Several mathematical treatments had been applied on BG resistivity equation in order to find semi-empirical relationship between integral constant and Debye temperature in noble materials as a

✉ E. Ching-Prado
  eleicer.ching@utp.ac.pa

1 Natural Science Department, Faculty of Science and Technology, Technological University of Panama, Victor Levy Sasso Campus, Panama City, Panama

function of temperature [19]. Thus, an electrical resistance study of thin ITO films has been described by the BG law with high two dimensional electron–electron interaction at very low temperature [20]. Also, CVD fluorine doped TO thin film has been found that its resistivity caused by the thermal phonons obeys BG model [21].

In this paper FTO thin film on glass substrate has been prepared by spray pyrolysis technique and discussed its optical and electrical properties, for first time, in terms of the Drude-Lorentz model, that to the best of our knowledge it is also the first time that both properties of a TCO are fitted simultaneously. While the FTO temperature dependence electrical behavior is analyzed in terms of Mathiessen's rule [18, 22]. In addition, a first principle calculation has been realized in order to understand, from a theoretical point of view, the experimental results from Density Functional Theory (DFT) approach. Finally, the FTO film was evaluated as a transparent electrode in a dye-sensitized solar cell.

2 Theory and calculation

The Drude-Lorentz theory formalisms that have been found to describe TCO optical and electrical properties can be shown to yield the following relationship for the frequency dependence for the complex permittivity [15]:

$$\varepsilon(\omega) = \varepsilon_\infty - \frac{\omega_p^2}{\omega^2 + i\gamma\omega} + \sum_k \frac{\omega_{pk}^2}{\omega_{ok}^2 - \omega^2 - i\gamma_k\omega} \qquad (1)$$

where ε_∞ represents the high-frequency dielectric constant and the parameters ω_{pk}, ω_{ok} and γ_k are the plasma frequency, the transverse frequency and the damping constant respectively of the k-th Lorentz oscillator. In the Drude model ω_p and γ have similar meaning as those of Lorentz contribution. So that the complex permittivity can be written as [14]:

$$\varepsilon(\omega) = \varepsilon_1(\omega) + i\varepsilon_2(\omega)$$

As it is known, this expression can be related to different optical parameters, such as the complex refraction index and the complex optical conductivity. Also, several dc electrical parameters can be related to the Drude's dielectric function contribution. Thus, the dc resistivity can be calculated with the expression [16]:

$$\rho = \frac{\gamma}{2\pi c\varepsilon_o\omega_p^2}$$

where c is the light speed and ε_o is the free space permittivity. Also, the carrier concentration (n) and the mobility (μ) can be obtained by the following relations [16]:

$$n = \frac{4\pi^2c^2\varepsilon_o m^*}{e^2}\omega_p^2$$

and

$$\mu = \frac{e}{2\pi m^* c\gamma}$$

where e is electron charge and $m^* = 0.28m_e$ (m_e the rest electron mass) is the effective mass reported for FTO [23]. Thus, the electron mean free path (ℓ) can be calculated using n and μ.

In addition, the film degeneracy can be evaluated through n by calculating the Fermi energy position relative to the conduction band minimum. It is called the Burstein–Moss shift ΔE_{BM} [24].

3 Experimental details

The precursor materials used to prepare fluorine doped tin oxide were dehydrate stannous chloride ($SnCl_2 \cdot 2H_2O$) and ammonium fluoride (NH_4F). A starting solution was obtained by mixing the precursors with distilled water and hydrochloric acid (HCl) of the following form: 6.0 g of $SnCl_2 \cdot 2H_2O$ was dissolved in 90 ml distilled water. After, 12 ml of HCl and 10 wt% NH_4F are added to the solution and it is stirred for 1 h. The final result is a solution completely homogeneous and transparent.

This solution was sprayed onto a heat glass plate using a semi-automated homemade spray pyrolysis system, see Fig. 1. The deposition temperature was 500 °C for 10 min and a source-substrate distance of 30.0 cm. After deposition, the film was allowed to cool to room temperature.

The surface morphologies of the film were analyzed at room temperature using a Scanning Electron Microscope (SEM) Zeiss Evo 40 vp. For optical characterization, an UV–Visible spectrometer model V-670 from Jasco was utilized in wavelength range of 200–1100 nm. The
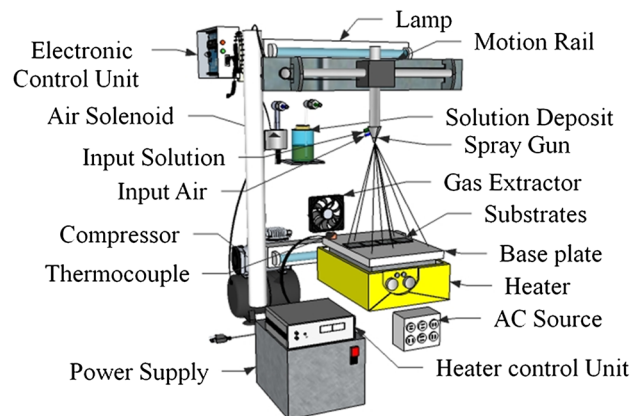

Fig. 1 Semi-automated home-made spray pyrolysis system

transmittance spectrum was fitted using ReFfit Program code [25, 26].

The sheet resistance measurements were performed by four-point Van der Pauw method. Silver epoxy paste was employed to ensure good electrical contacts. A temperature dependence study of the electrical response was realized using a Peltier cell in temperature range from 278 to 403 K.

4 Results and discussion

Figure 2a presents the SEM micrograph of the FTO thin film. It is compact and adherent in nature. Homogeneous and well define grains can be observed, which indicates the polycrystalline nature of the sample. The inset figure shows the grain size histogram obtained through a standard image analysis process. Thus, a grain size distribution from 16 to 380 nm was found, with an average value of 155 nm. The X-ray diffraction pattern observed to the FTO film (Fig. 2b) presents bands associated to planes whose Miller´s indices are (110), (101), (200), etc. They are all characteristics of the
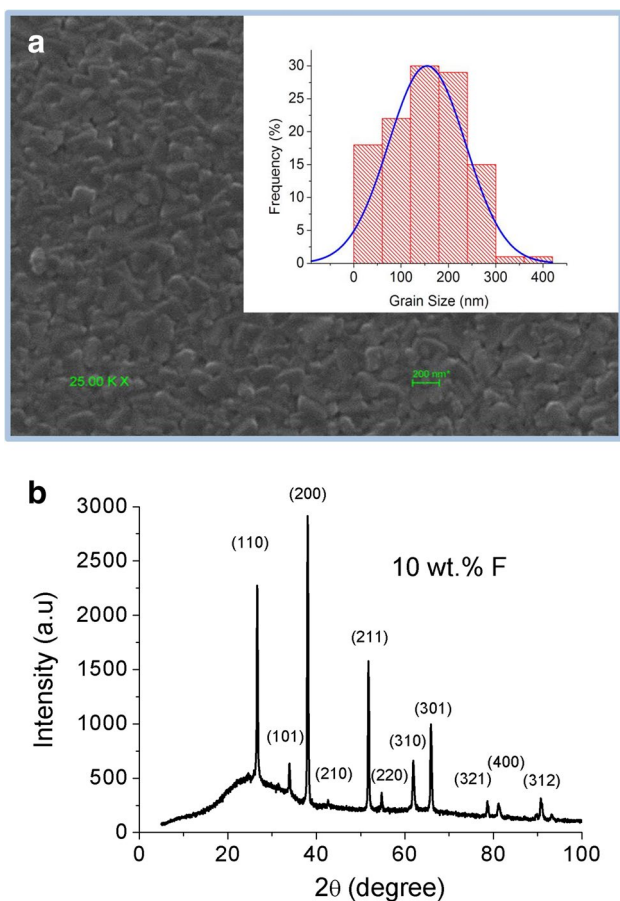
well known tetragonal-rutile structure. The obtained rutile phase is comparable with the standard SnO_2 (TO) material, Card No. 88-0287 from JCPDS data. It corresponds to a material structure with P42/mnm space group. But, it is expected that the presence of fluorine atoms must break the structural symmetry. However, a similar XRD diagram is found between TO and FTO materials. It is due to the very close ionic radii between oxygen (1.36 Å) and fluorine (1.30 Å) with an atom coordination number of three.

Figure 3 shows the optical transmittance spectrum of FTO on glass substrate. The well-developed fringes pattern in transmittance indicates that the film has a smooth surface with well define air-FTO and FTO-glass substrate interfaces [27]. In addition, the good interference behavior shows that the film is morphologically homogeneous, and this is in agreement with the scanning electron microscope picture obtained of the sample. As shown in Fig. 3, the sample exhibit sharp absorption edges at 290–350 nm, indicating the high quality of the crystallites. The average transmission in the visible region has been found to be 81.2%.

This FTO/glass spectrum is fitted using Drude-Lorentz model, which is a multilayer's classical dispersion theory. Thus, Fig. 3 shows the fitted transmittance spectrum for the FTO sample; where the Van der Pauw conductivity measurement has been considered a condition in the fitting process, see Fig. 4. A very good result was obtained and the Table 1 presents the fitted spectrum parameters. It can be observed, in Fig. 4, that the real part optical conductivity presents four (4) bands with maximum at 0 (0 eV), 24,061 cm^{-1} (3.0 eV), 29,214 cm^{-1} (3.6 eV) and 32,315 cm^{-1} (4.01 eV). These features also appear, as expected, in others optical parameters and they will be discussed in the next paragraph. In addition, Fig. 3 shows the theoretical FTO reflectance spectrum obtained using the fitted parameters, which it is in perfect
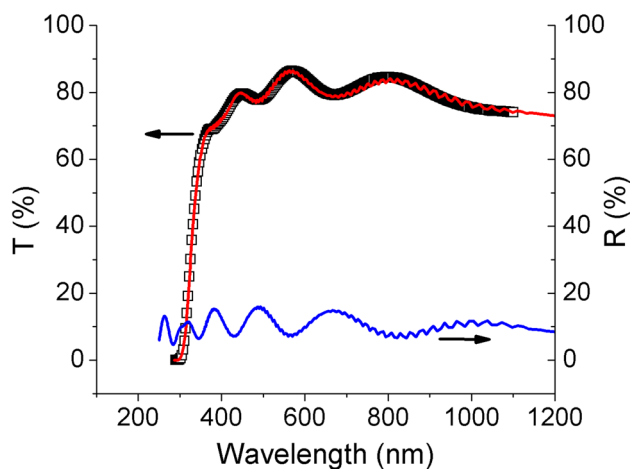

Fig. 2 a SEM micrograph of FTO thin film deposited on glass substrate. **b** XRD diffraction pattern of FTO thin film deposited on glass substrate

Fig. 3 Measured and simulated FTO transmittance spectra. The reflectance spectrum is obtained using the dielectric function fitting parameters
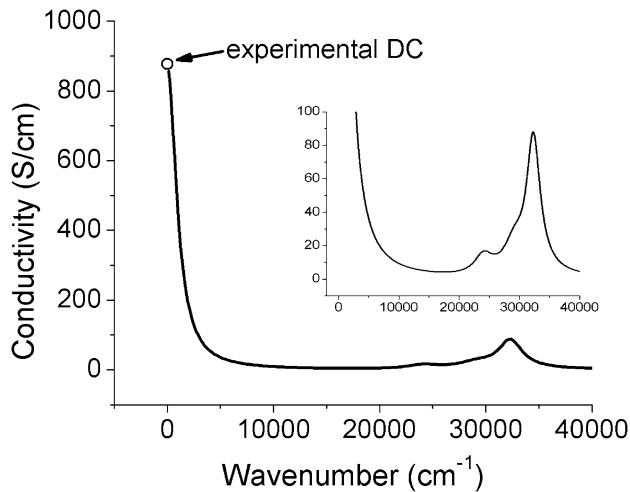
Fig. 4 Electrical conductivity of FTO thin film. The open dot point in zero (0) wavenumber corresponds to DC conductivity value measured by Van der Pauw technique, and it is a fitting condition. The solid line is the conductivity frequency dependency obtained by the dielectric function parameters

Fig. 5 Real and imaginary dielectric functions of FTO thin film

agreement with the experimental spectrum reported in the literature [3, 28]. So, the frequency dependence of the dielectric function and many others optical properties can be determined completely in the UV–Visible range.

Figure 5 shows the real and imaginary parts of the dielectric function for FTO layer. Three main features are observed in this figure. (1) At low energy, around 0–2.0 eV, the sharp increase and decrease for the real and imaginary parts respectively is due to the intra-band transitions of electrons in the conduction band and close to the Fermi level, corresponding to a metal-like behavior and described by the Drude model. (2) The increase at high energies, around 4.01 eV is related to the optical band gap transitions [15], and (3) The two soft increases at 3.0 and 3.6 eV are described by Lorentz oscillators and they seem to be related to a trap created inside of the band gap and close to the conduction band, as a consequence of oxygen vacancies [29]. In order to prove this, without the presence of fluorine, a TO thin film sample was prepared with the same FTO spray pyrolysis condition, where a high oxygen vacancy
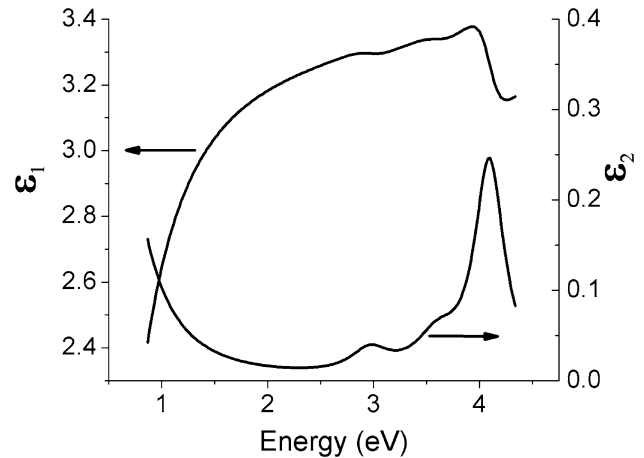
concentration is known to take place when TO is prepared as a TCO material. Table 1 shows the Drude-Lorentz fitting parameters of TO thin film, where two soft features lower to the optical band gap, around 18,461 cm^{-1} (2.29 eV) and 24,817 cm^{-1} (3.07 eV), can be observed. Thus, the 3.0 eV found in FTO thin film clearly corresponds to electron transition from the valence band to the defect level (trap) inside of the band gap due to oxygen vacancies. If this transition involves the VBM, then the defect level is found around to 0.62 eV under the conduction band minimum. In this approach, the 3.6 eV band can also be explained as a transition from deeper valence band (0.6 eV under VBM) to the defect level.

Table 2 shows the calculated resistivity, carrier concentration, mobility, mean free path, optical band gap and relative Fermi level using the fitted dielectric function parameters. A resistivity value of 1.15×10^{-3} Ω-cm is obtained, which it is in good agreement with 1.14×10^{-3} Ω-cm found experimentally. A carrier concentration of 1.70×10^{20} cm^{-3} and a mobility of 32.05 cm^2/Vs are obtained and they are similar to those with good electrical properties reported in the literature [30]. The FTO film shows a mean free path of 36.20 Å. It is considerably shorter than the 155 nm average grain size measured by SEM. This indicates that the mobility is limited

Table 1 Fitting parameters of FTO thin film using Drude-Lorentz model. It includes the film thickness d

Samples	ε_∞	ω_p (cm^{-1})	γ (cm^{-1})	k	ω_{0k} (cm^{-1})	ω_{pk} (cm^{-1})	γ_k (cm^{-1})	d (nm)
FTO	3.33	7363	1038.4	1	24,061	1598.6	3717.2	475
				2	29,214	2144.3	4283.5	
				3	32,315	3616.7	2716.4	
TO	2.97	5461.8	2331.5	1	18,461	1262.3	4755.4	462
				2	24,817	1945.4	4996.7	
				3	35,492	11,035	5977.9	

*Experimental result

Table 2 FTO electrical and optical parameters calculated using Drude model

Sample	$\rho \times 10^{-3}$ (Ω-cm)	$n \times 10^{20}$ (cm^{-3})	μ (cm^2/Vs)	ℓ (Å)	E_g^o (eV)	ΔE_{BM} (eV)
FTO	1.15 (1.14)*	1.70	32.05	36.20	4.01	0.40

*Experimental result

by scattering of the ionized fluorine atoms and others bulk structural defects rather than scattering of the grain boundary. The calculated relative Fermi energy (Burnstein–Moss effect) is 0.40 eV, which is higher than the room temperature thermal energy (KT = 0.025 eV). It evidences the degenerate nature of the FTO film. Thus, the 4.01 eV optical band gap corresponds to electron transition from valence band to lowest unoccupied conduction band. This optical transition energy is given by the following expression [24]:

$$E_g^o = E_g + \Delta E_{BM} - \Delta E^{BGN}$$

where E_g corresponds to the intrinsic TO band gap, with experimental value reported in the literature around 3.62 eV. While ΔE^{BGN} is the band gap shrinkage usually results from scattering against ionized impurities and the correlated motion of charged carriers. The results seem to indicate that the ΔE^{BGN} term is very small (around 0.01 eV). So that, the well documented renormalization of the host band gap in degenerate doping semiconductor seems not to take place practically. It suggests that most of the scattering process is due to bulk structural defect, such as vacancy and atoms in non-equilibrium position, than due only to fluorine impurity. However, it seems contradictory with the amount of fluorine used in the starting solution. So that, it probably indicates that the presence of fluorine in the FTO thin film is much less than that in the precursor solution, as it has also been observed by other researchers [4, 31, 32].

Figure 6 shows the electrical resistivity behavior of the FTO film from 278 to 403K. According to Mathiessen's rule the electrical resistivity in many materials can be expressed as a sum of the residual and the temperature-dependent resistivity contributions.

$$\rho(T) = \rho(0) + \rho_{el-ph}(T) + \rho_{el-el}(T) + \dots \quad (2)$$

where $\rho(0)$ corresponds to the residual resistivity, $\rho_{el-el}(T)$ is the electron–electron interaction, and $\rho_{el-ph}(T)$ is the electron–phonon interaction given by BG model [18, 22].

$$\rho_{el-ph}(T) = \beta T \left(\frac{T}{\theta_D} \right)^4 \int_0^{\frac{\theta_D}{T}} \frac{x^5 dx}{(e^x - 1)(1 - e^{-x})} \quad (3)$$

where $x = \hbar\omega/K_B T$, β is a constant and θ_D is the Debye temperature.

It can be observed that no good fitting is obtained using Eq. (2), with the two first terms, and Eq. (3). So that, the electrical responses do not obeys the BG model on this
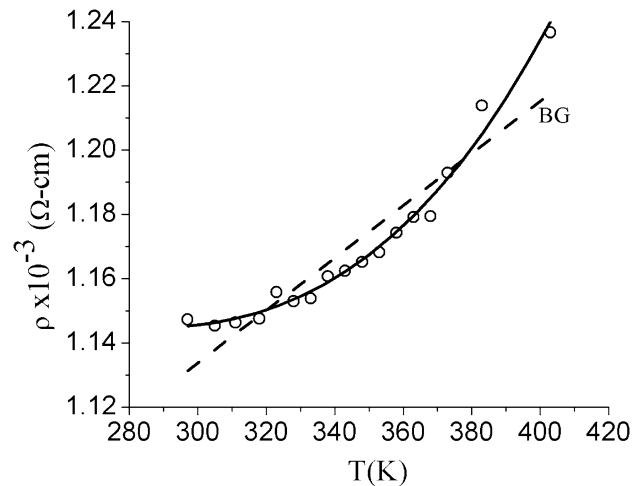

Fig. 6 Temperature dependence of dc electrical resistivity in FTO thin film. The dash line is the fitting using BG equation. The solid line is the fitting using the polynomial $\rho(T) = \rho(0) + \alpha T^2 + \beta T^5$

temperature range as it has been found in others metal oxide materials. However, a good result is found with the expression $\rho(T) = \rho(0) + \alpha T^2 + \beta T^5$, where α and β are constants. The second term can be associated with electron–electron interaction, while the third term is the electron–phonon interaction for temperature higher than Debye temperature. Thus, the little variation of the electric resistivity with the temperature indicates that the residual contribution, which is temperature independent, is the most important term. It corresponds to an electron–defect interaction. This result is in perfect agreement with the small electron mean free path value obtained before.

In order to understand from a theoretical point view the inclusion of F atoms in TO structure a DFT first-principles approach was implemented within the Quantum Espresso computer code [33]. The hybrid functional PBE0 is adopted for describing the exchange-correlation interactions [34]. Figure 7a shows the electronic density of state (DOS) of dielectric TO with well defined direct band gap ($E_g = 3.62$ eV), where the Fermi level is found in the valence band maximum (VBM) as expected. This means that the conduction bands are completely unoccupied and the material exhibits electrical insulation property. This DOS result is in perfect agreement with the experimental low energy high resolution XPS measurement [35], which indicates that our DFT theoretical approach is correct. Thus, Fig. 7b shows the DOS for a FTO sample with fluorine concentration of 8.33 at.%. It can
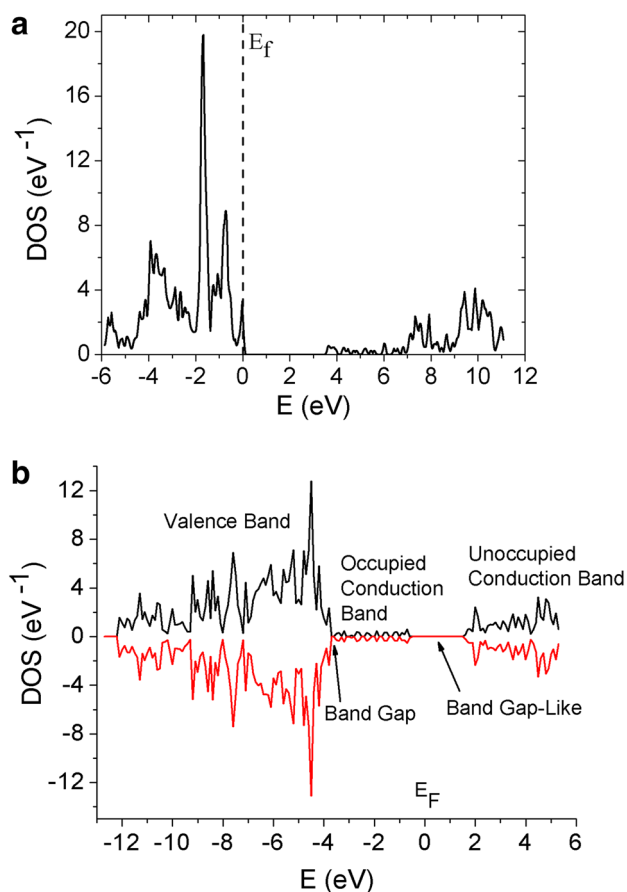
Fig. 7 a Electronic density of state (DOS) of TO by DFT first principle calculation. **b** DOS of FTO structure with 8.33 at.% fluorine concentration. All the energy values are relatives to the Fermi level (E_F). The positive DOS value (black) corresponds to spin up structure, while the negative DOS (red) corresponds to spin down structure. (Color figure online)

Fig. 8 Density of current–voltage curve for FTO film utilized as electrode in the dye-sensitized solar cells (DSSCs). Inset the quantum efficient spectrum

be observed that the Fermi level is in the conduction band region with Burstein-Moss shift of 3.47 eV, band gap of 0.33 eV and optical band gap of 5.24 eV. So, the theoretical sample (TS) exhibits TCO's properties. Also, inside the conduction bands a band gap like-behavior can be observed with energy value around 2.00 eV. A complete FTO theoretical study (not shown here) indicates that the band gap and the band gap like behavior decrease and increase with increasing F content, respectively. Thus, inter-band transitions from occupied to unoccupied conduction bands can take places. Therefore, transition bands with energy lower than the optical band gap are possible with introducing F content in TO structure. So, they can also contribute to the two lorentzian oscillators corresponding to transitions at 3.0 and 3.6 eV, obtained in UV–Visible experimental measurements and discussed above only in term of oxygen vacancies.

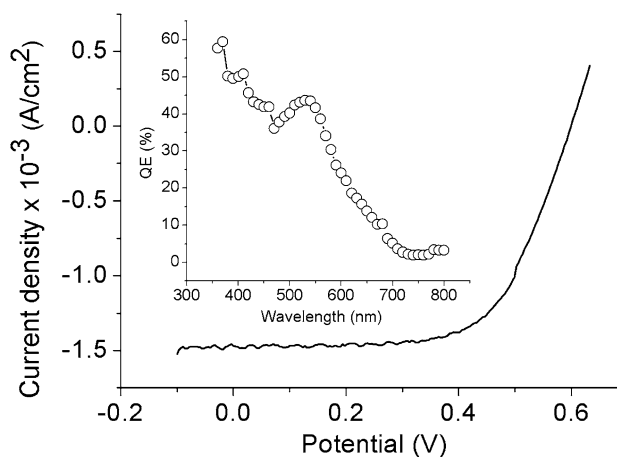Also, the FTO sample was utilized as an electrode in the preparation of a dye-sensitized solar cell (DSSCs). For

fabrication of DSSCs, the FTO film was coated with a compact 800 nm-TiO_2 film by spray pyrolysis method and after with a 4 μm-TiO_2 nanoparticles layer using Doctor Blade technique. The electrode was immersed in the commonly used dye-N719 (0.2 mM) with soaking time of 24 h. The photovoltaic parameters indicate a short-circuit current density of Jsc = 12.3 mA/cm2, an open-circuit voltage of Voc = 0.60 V, a fill factor of ff = 63.5%, a power conversion efficiency of η = 4.7% and a quantum efficient QE = 43% at 535 nm (see Fig. 8).

5 Conclusions

Thin film of FTO was prepared by spray pyrolysis technique. The real and imaginary dielectric functions show an intra-band transition in the conduction band corresponding to free-like electron, which it is modeled with Drude theory. Thus, the calculated relative Fermi energy (Burnstein–Moss effect) reveals the degenerate nature of the FTO film. While the electron mean free path indicates that the electron mobility is limited by scattering of the ionized fluorine atoms and others bulk structural defects rather than scattering of the grain boundary.

Also, a 4.01 eV feature in the UV–Visible spectrum is related to optical band gap associated to direct inter-band transition, from the valence band to the lowest unoccupied conduction band, out of the Brillouin zone center. Additionally, two optical transitions at 3.0 and 3.6 eV associated to oxygen vacancies are obtained using Lorentz model. They seem to correspond to transitions from VBM and deeper valence band to a defect level close to the conduction band, respectively. The density functional theory shows that inter-band transitions from occupied conduction band

to unoccupied conduction band are possible, and they can contribute to the two optical transitions mention before. In addition, a power conversion efficiency of $\eta = 4.7\%$ is found in a dye-sensitized solar cell when the FTO thin film is used as a transparent electrode.

It can be noted that no empirical process is utilized to analyze the optical and electrical measurements of FTO thin film at room temperature, as it is found in many others papers. An analytical classical dispersion theory has been used in this study for obtaining optical and electrical parameters simultaneously. After, a first principle calculation, through DFT method, is realized to SnO_2 and FTO material in order to explain optical transitions with its respective electronic bands structure.

References

1. R. Babar, S.S. Shinde, A.V. Moholkar, C.H. Bhosale, J.H. Kim, K.Y. Rajpure, Physical properties of sprayed antimony doped tin oxide thin films thickness: the role of thickness. J. Semicond. **32**(5), 053001–053001 (2011)

2. E. Ching-Prado, A. Watson, H. Miranda, I. Abrego, Optical properties of multilayers TiO_2/SnO_2:F thin films. MRS Adv. (Energy and Environment). **1**(46), 3133 (2016)

3. B. Zhang, J. Tian, J.X. Zhang, W. Cai, The studies on the role of fluorine in SnO_2:F films prepared by spray pyrolysis with $SnCl_4$. J. Optoelectron. Adv. Mater. **13**(1), 89 (2011)

4. Z.Y. Banyamin, P.J. Kelly, G. West, J. Boardman, Electrical and optical properties of fluorine doped tin oxide thin films prepared by magnetron sputtering. Coatings **4**, 732 (2014)

5. J.M. Rodríguez, A. Watson, I. Abrego, J. Ardisson, C.A. Samudio, E. Ching-Prado, A water vapor sensor application of $Sn_{1−x}Fe_xO_{2−d}$. Mater. Res. Soc. Symp. Proc. (2015). https://doi.org/10.1557/opl.2015.788

6. A.A. Yadava, E.U. Masumdar, A.V. Moholkar, M. Neumann-Spallart, K.Y. Rajpure, C.H. Bhosale, Electrical, structural and optical properties of SnO_2:F thin films: effect of the substrate temperature. J. Alloy. Compd. **488**, 350 (2009)

7. A. Agashe, S. Mahamuni, Competitive effects of film thickness and growth rate in spray pyrolytically deposited fluorine-doped tin dioxide films. Thin Solid Films **518**, 4868–4873 (2010)

8. K. Kaviyarasu, P.A. Devarajan, S.S.J. Xavier, S.A. Thomas, S. Selvakumar, One pot synthesis and characterization of cesium doped SnO_2 nanocrystals via a hydrothermal process. J. Mater. Sci. Technol. **28**(1), 15–20 (2012)

9. M. Arularasu, M. Anbarasu, S. Poovaragan, R. Sundaram, K. Kanimozhi, C.M. Magdalane, K. Kaviyarasu, F. Thema, D. Letsholathebe, G.T. Mola, M. Maaza, Structural, optical, morphological and microbial studies on SnO_2 nanoparticles prepared by co-precipitation method. J. Nanosci. Nanotechnol. **18**(5), 3511–3517 (2018)

10. J. Kennedy, P.P. Murmu, E. Manikandan, S.Y. Lee, Investigation of structural and photoluminescence properties of gas and metal ions doped zinc oxide single crystals. J. Alloy. Compd. **616**, 614–617 (2014)

11. J. Kennedy, P.P. Murmu, J. Leveneur, A. Markwitz, J. Futter, Controlling preferred orientation and electrical conductivity of zinc oxide thin films by post growth annealing treatment. Appl. Surf. Sci. **367**, 52–58 (2016)

12. E. Sathyaseelan, K. Manikandan, J. Sivakumar, M. Kennedy, Maaza, Enhanced visible photoluminescent and structural properties of ZnO/KIT-6 nanoporous materials for white light emitting diode (w-LED) application. J. Alloy. Compd. **651**, 479–482 (2015)

13. K. Kaviyarasu, C.M. Magdalane, K. Kanimozhi, J. Kennedy, B. Siddhardha, C.S. Sharma, F.T. Thema, E.S. Reddy, N.K. Rotte, D. Letsholathebe, G.T. Mola, M. Maaza, Elucidation of photocatalysis, photoluminescence and antibacterial studies of ZnO thin films by spin coating method. J. Photochem. Photobiol. B **173**, 466–475 (2017)

14. I. Chambouleyron, J.M. Martínez, in *Optical Properties of Dielectric and Semiconductor*, Chap. 12, ed. by H.S. Nalwa. Handbook of Thin Films Materials, vol. 3 (Academic Press, San Diego, 2001), pp. 1–30

15. M. Kadi, A. Smaali, R. Outemzabet, Analysis of optical and related properties of tin oxide thin films determined by Drude-Lorentz model. Surf. Coat. Technol. **211**, 45 (2012)

16. B.V. Odari, M. Mageto, R. Musembi, H. Othieno, F. Gaitho, V. Muramba, Optical and electrical properties of Pd doped Sno_2 thin films deposited by spray pyrolysis. Aust. J. Basic Appl. Sci. **7**(2), 89–98 (2013)

17. F.C. Lai, L.M. Lin, R.Q. Gai, Y.Z. Lin, Z.G. Huang, Determination of optical constants and thicknesses of In_2O_3:Sn films from transmittance data. Thin Solid Films **515**, 7387 (2007)

18. J. Lin, Z.Q. Li, Electronic conduction properties of indium tin oxide: single-particle and many-body transport. J. Phys. **26**, 343201–343201 (2014)

19. M.A. Al-Jalali, S.A. Mouhammad, Phonons Bloch-Gruneisen function and its applications to noble metals resistivity. Int. J. Pure Appl. Math. **102**(2), 233 (2015)

20. B.-T. Lin, Y.-F. Chen, J.-J. Lin, C.-Y. Wu, Temperature dependence of resistance and thermopower of thin indium tin oxide film. Thin Solid Films **518**, 6997 (2010)

21. H. Gao, T. Lin, X.D. Liu, X.H. Zhang, X.N. Li, J. Wu, Y.F. Liu, X.F. Wang, Y.W. Chen, N. Ni, N. Dai, J.H. Chu, Low temperature electrical transport properties of F-doped SnO_2 films. Solid State Commun. **157**, 49 (2013)

22. G. Utlu, N. Artunc, The effects of grain boundary scattering on electrical resistivity of Ag/NiSi silicide films formed on silicon substrate at 500 °C by RTA. Appl. Surf. Sci. **310**, 248 (2014)

23. H. Cachet, in *Films and Powders of Fluorine-Doped Tin Dioxide*, 1st edn, ed. by T. Nakajima, H. Groult. Fluorinated Materials for Energy Conversion (Elsevier Science, Amsterdam, 2005), p. 520

24. Y. Dou, T. Fishlock, R.G. Egdell, Band-gap shrinkage in *n*-type-doped CdO probed by photoemission spectroscopy. Phys. Rev. B **55**(20), R13381 (1997)

25. A.B. Kuzmenko, Kramers Kronig constrained variational analysis of optical spectra. Rev. Sci. Instrum. **76**(8), 083108 (2005)

26. B. Kuzmenko, Guide to Reffit (2004). http://optics.unige.ch/alexey/reffit.html. Accessed 7 Jan 2016

27. G. Kaur, A. Mitra, K.L. Yadav, Pulsed laser deposited Al-doped ZnO thin films for optical applications. Progr. Nat. Sci. **25**(1), 12 (2015)

28. A.R. Babar, S.S. Shinde, A.V. Moholkar, C.H. Bhosale, K.Y. Rajpure, Structural and optoelectronic properties of sprayed Sb:SnO_2 thin films: effects of substrate temperature and nozzle-to-substrate distance. J. Semicond. **32**(10), 102001–102001 (2011)

29. F. El Akkad, T.A.P. Paulose, Optical transitions and point defects in F:SnO_2 films: effect of annealing. Appl. Surf. Sci. **295**, 8 (2014)

30. E. Elangovan, K. Ramamurthi, Studies on micro-structural and electrical properties of spray-deposited fluorine-doped tin oxide

thin films from low-cost precursor. Thin Solid Films **476**, 231 (2005)

31. W.Z. Samad, M.M. Salleh, A. Shafiee, M.A. Yarmo, Structural, optical and electrical properties of fluorine doped tin oxide thin films deposited using inkjet printing technique. Sains Malaysiana **40**(3), 251 (2011)

32. T. Fukano, T. Motohiro, Low-temperature growth of highly crystallized transparent conductive fluorine-doped tin oxide films by intermittent spray pyrolysis deposition. Sol. Energy Mater. Sol. Cells. **82**, 567 (2004)

33. P. Giannozzi, S. Baroni, N. Bonini, M. Calandra, R. Car, C. Cavazzoni, D. Ceresoli, G.L. Chiarotti, M. Cococcioni, I. Dabo, A. Dal Corso, S. Fabris, G. Fratesi, S. de Gironcoli, R. Gebauer, U. Gerstmann, C. Gougoussis, A. Kokalj, M. Lazzeri, L. Martin-Samos, N. Marzari, F. Mauri, R. Mazzarello, S. Paolini, A. Pasquarello, L. Paulatto, C. Sbraccia, S. Scandolo, G. Sclauzero, A.P. Seitsonen, A. Smogunov, P. Umari, R.M. Wentzcovitch, QUANTUM ESPRESSO: a modular and open-source software project for quantum simulations of materials. J.Phys. **21**(1), 395502 (2009)

34. J.P. Perdew, M. Ernzerhof, K. Burke, Rationale for mixing exact exchange with density functional approximations. J. Chem. Phys. **105**(22), 9982 (1996)

35. M. Weidner, Fermi level determination in tin oxide by photoelectron spectroscopy, Thesis, Technischen Universität *Darmstadt*, Germany (2016)